

Measurements of the Thermal Conductivity of HFC-125 in the Temperature Range from 300 to 515 K at Pressures up to 53 MPa

B. Le Neindre^{1,2} and Y. Garrabos³

Received July 9, 1998

Measurements of the thermal conductivity of HFC-125 that have been made by a coaxial cylinder cell operating in steady state are reported. The measurements of the thermal conductivity of HFC-125 were performed along several quasi-isotherms between 300 and 515 K in the gas phase and the liquid phase. The pressure range covered varies from 0.1 to 53 MPa. Based on the measurement of more than 600 points, an empirical equation is provided to describe the thermal conductivity outside the critical region as a function of temperature and density. A careful analysis of the various sources of error leads to an estimated uncertainty of approximately $\pm 1.5\%$.

KEY WORDS: coaxial cylinders; high pressure; refrigerants; HFC-125; thermal conductivity.

1. INTRODUCTION

Recently the thermophysical properties of HFC-125 (pentafluoroethane) have been investigated widely since this hydrofluorocarbon is expected to be an environmentally acceptable alternative to the refrigerant HCFC-22 (chlorodifluoromethane), used in refrigeration, heat pumps, and air-conditioning equipment, either as a pure compound or in a mixture. Previous measurements of the thermal conductivity of HFC-125, which were carried

¹ LIMHP-CNRS, Institut Galilée, Université Paris Nord, Av. J. B. Clément, 93430 Villetaneuse, France.

² To whom correspondence should be addressed.

³ Institut de Chimie de la Matière Condensée de Bordeaux, Université de Bordeaux I, Av. du Dr. Schweitzer, 33608 Pessac, France.

out mostly in the liquid phase, revealed significant discrepancies from each other that are much larger than the uncertainties claimed by the respective authors. The thermal conductivity of HFC-125 was measured in a vertical coaxial cylinder cell, operating in the steady-state mode. We have investigated the influence of temperature and pressure on the thermal conductivity. The measurements were performed to make an analysis of the data based on the residual concept. The thermal conductivity $\lambda(T, \rho)$ is a function of temperature T and density ρ that may be represented as the sum of three terms:

$$\lambda(T, \rho) = \lambda_0(T) + \delta\lambda(T, \rho) + \Delta\lambda(T, \rho) \quad (1)$$

where $\lambda_0(T)$ is the dilute gas thermal conductivity, $\delta\lambda(T, \rho)$ is the residual thermal conductivity, and $\Delta\lambda(T, \rho)$ is the critical enhancement. The dilute gas contribution $\lambda_0(T)$ was obtained by performing measurements at atmospheric pressure as a function of temperature. The background term,

$$\lambda_B(T, \rho) = \lambda_0(T) + \delta\lambda(T, \rho) \quad (2)$$

was obtained by making measurements along quasi-isotherms as a function of pressure in the liquid phase and in the gas phase far away from the critical region. The remaining contribution, $\Delta\lambda(T, \rho)$, represents the enhancement of the thermal conductivity due to critical fluctuations and becomes significant in the supercritical region or in the subcritical region along the saturation curve. In this paper, we report only experimental data in the liquid phase and in the gas phase far away from the critical point in order to determine the so-called thermal conductivity background. Our measurements in the critical region and in the gas phase below the critical point will be reported later. The density was calculated with an equation of state reported by Outcalt and McLinden [1], where the critical parameters are given as follows: $T_c = 339.33$ K, $p_c = 3.629$ MPa, and $\rho_c = 571.29$ kg · m⁻³.

2. EXPERIMENTAL APPARATUS

The thermal conductivity of HFC-125 was measured using vertical coaxial cylinders operating in the steady-state mode. The same device was already used in the measurement of the thermal conductivity of 1-chloro-1,1-difluoroethane (HCFC-142b) [2]. A detailed description of the cell and of the method of measurement is available [3]. The sample was provided by Elf Atochem, and its purity was estimated to be better than 99.8% by the manufacturer's analysis.

3. DILUTE-GAS THERMAL CONDUCTIVITY

The results of the measurement of the thermal conductivity at atmospheric pressure are listed as a function of temperature in Table I. The experimental data were fitted by a linear equation:

$$\lambda_0 = -11.1 + 0.0840T \quad (3)$$

Figure 1 shows the deviations between experimental data reported in this work and Eq. (3). The temperature dependence of the thermal conductivity of the dilute gas can be represented by an expression derived from the kinetic theory of gases. The thermal conductivity is related to the reduced effective collision cross sections, which contain all the contributions of translational, rotational, vibrational, and electronic degrees of freedom. As there is a lack of reliable experimental data on the vibrational collision number, for the calculation of the thermal conductivity at zero density, we used the practical engineering form:

$$\lambda_0(T) = \frac{0.177568(T/M)^{0.5} C_p^0/R}{\sigma^2 \Omega_\lambda^*} \quad (4)$$

where Ω_λ^* is the reduced effective collision cross section for thermal conductivity and C_p^0 is the ideal isobaric heat capacity.

The scaling factors, σ and ε/k , which correspond to the effective Lennard-Jones 12-6 potential parameters, were determined by a regression analysis of both viscosity and thermal conductivity data at atmospheric pressure. For this purpose the experimental viscosity data (in $\mu\text{Pa}\cdot\text{s}$) [4-6] near atmospheric pressure were represented by a linear equation:

$$\eta_0 = 1.04 + 0.04T \quad (5)$$

Table I. Thermal Conductivity of HFC-125 at Atmospheric Pressure

T (K)	λ (mW · m ⁻¹ · K ⁻¹)	T (K)	λ (mW · m ⁻¹ · K ⁻¹)	T (K)	λ (mW · m ⁻¹ · K ⁻¹)
297.27	14.02	375.09	20.52	422.94	24.35
301.84	14.41	376.66	20.63	425.26	24.50
302.80	14.29	384.29	21.02	433.52	25.41
316.82	15.64	387.48	21.28	434.50	25.47
325.86	16.21	390.97	21.67	453.41	27.07
332.24	16.71	393.88	21.85	454.54	27.13
335.10	16.98	394.46	22.20	463.28	27.63
347.00	17.91	401.36	22.71	473.73	28.53
354.22	18.61	413.81	23.47	493.31	30.25
359.52	19.18	414.88	23.96	513.21	32.00

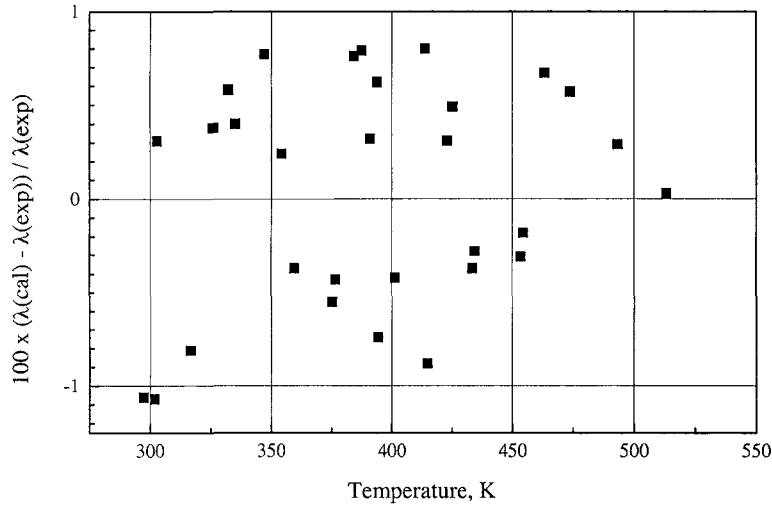


Fig. 1. Relative deviations between the calculated values of thermal conductivity [Eq. (3)] and the experimental data at atmospheric pressure.

The experimental viscosity data of Wilson et al. [4], Assael and Polimatidou [5], and Oliveira and Wakeham [6] are compared with Eq. (5) in Fig. 2. The best agreement between experimental data of both thermal conductivity and viscosity and calculated values by the corresponding theoretical equations was found for $\epsilon/k = 249$ K and $\sigma = 0.519$ nm. The ideal specific heat at constant pressure was calculated from the data reported by Yokozeki et al. [7]:

$$\frac{C_P^0}{R} = \sum_{i=0}^5 c_i T^i \quad (6)$$

where

$$\begin{aligned} c_0 &= 3.11482, & c_1 &= 0.029576 \\ c_2 &= 7.06976 \times 10^{-6}, & c_3 &= -6.033224 \times 10^{-8} \\ c_4 &= 5.6856726 \times 10^{-11}, & c_5 &= -1.727537 \times 10^{-14} \end{aligned}$$

The reduced collision integral Ω_λ^* was estimated as a function of reduced temperature, $T^* = kT/\epsilon$, using a functional expansion:

$$\Omega_\lambda^* = \sum_{j=1}^3 A_j (1/T^*)^j \quad (7)$$

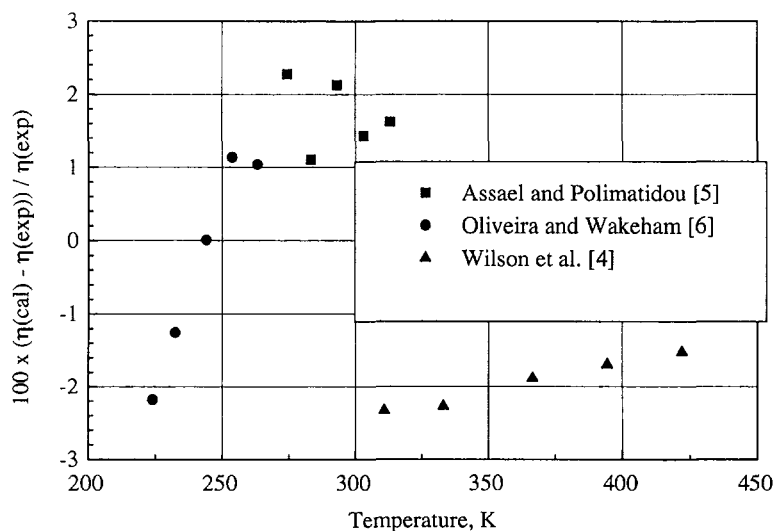


Fig. 2. Relative deviations between the calculated values of viscosity [Eq. (5)] and the experimental data at atmospheric pressure.

where

$$A_1 = 0.444358, \quad B_1 = 0.327867, \quad C_1 = 0.1936835$$

The deviations of the present experimental thermal conductivity data from their optimal representation by Eqs. (4), (6), and (7) are shown in Fig. 3. The percentage deviations between the experimental data fitted by Eq. (3) and the theoretical values calculated by Eqs. (4), (6), and (7) were found to be less than $\pm 1\%$ from 260 to 685 K. For the viscosity, the percentage deviation between experimental data fitted by Eq. (5) and calculated values using the potential parameters was found to be less than $\pm 1\%$ from 250 to 475 K, however, it increases significantly above 475 K and reaches -7% at 700 K. Moreover, the deviations are slightly larger if the theoretical values of the viscosity are compared to experimental ones, as shown in Fig. 4. The agreement with theory is very satisfactory for viscosity and thermal conductivity in the temperature range where experimental data are available. As shown in Fig. 5, the comparison between the values calculated by Eq. (3) and those of Assael et al. [8] near atmospheric pressure shows a mean deviation of $+1.5\%$, but the data of Tanaka et al. [9] are systematically 4% lower.

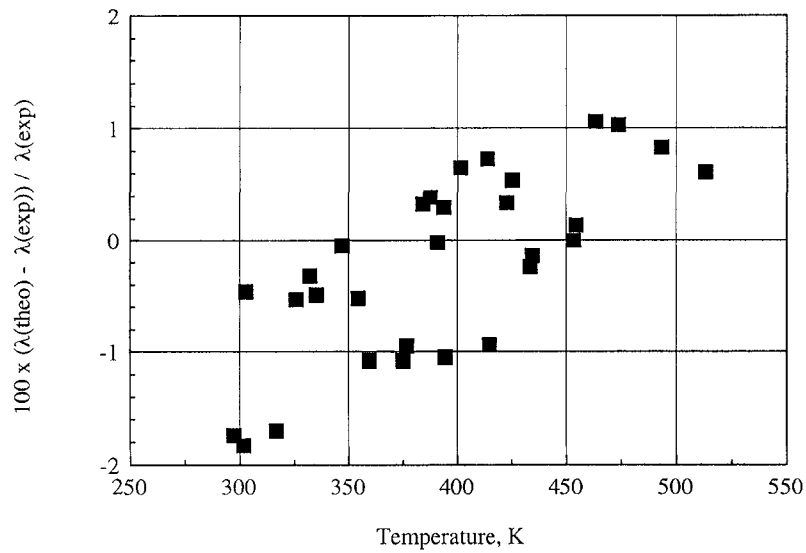


Fig. 3. Relative deviations between the theoretical values of the thermal conductivity [Eqs. (4) to (7)] and the experimental data at atmospheric pressure.

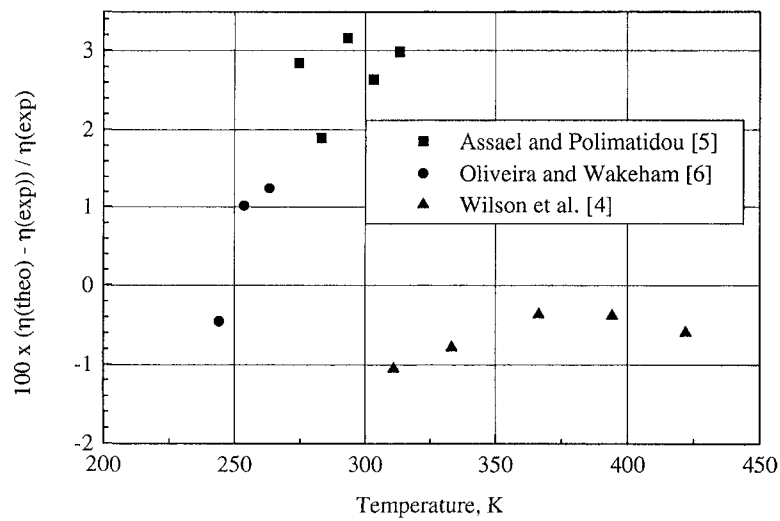


Fig. 4. Relative deviations of the theoretical values of viscosity from the experimental data at atmospheric pressure.

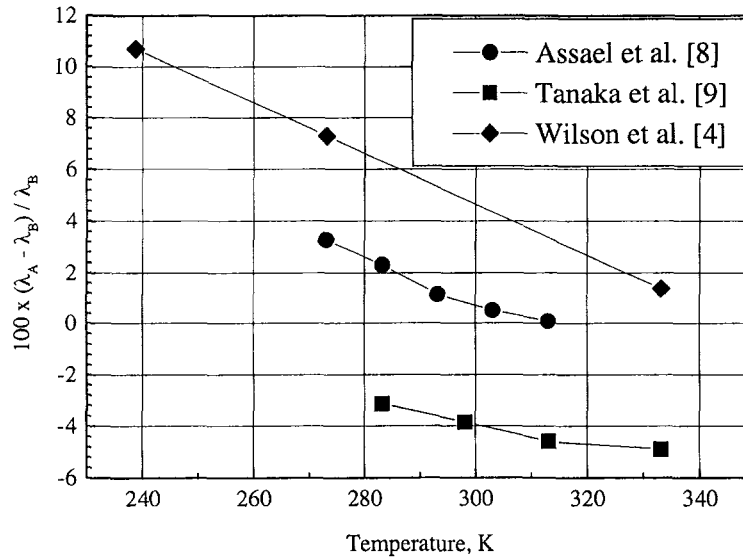


Fig. 5. Relative deviations of the experimental data at atmospheric pressure from the values calculated with the background equation.

4. DENSE FLUID THERMAL CONDUCTIVITY

In order to determine the excess function or the residual term of the thermal conductivity $\delta\lambda(\rho, T)$, we performed measurements in the liquid phase and in the supercritical gas phase far away from the critical region along 14 quasi-isotherms at 299, 300, 308.6, 317, 317.5, 327.2, 375, 424, 433, 453, 463, 473, 493, and 513 K. Experimental results are listed in Tables II to XV. The residual function for the thermal conductivity has been represented by a six-order polynomial of the form,

$$\frac{\delta\lambda}{A_c} = \sum_{i=1}^6 b_i \left(\frac{\rho}{\rho_c}\right)^i \quad (8)$$

where $\rho_c = 571.28 \text{ kg} \cdot \text{m}^{-3}$ is the critical density, and the coefficients b_i in Eq. (8) are

$$\begin{aligned} b_1 &= 6.180883 \times 10^{-4}, & b_2 &= 2.7278622 \\ b_3 &= -3.33142, & b_4 &= 2.181201 \\ b_5 &= -0.6624914, & b_6 &= 8.123548 \times 10^{-2} \end{aligned}$$

and $A_c = 13.3 \text{ mW} \cdot \text{m}^{-1} \cdot \text{K}^{-1}$.

The comparison with the data of Assael and Karagiannidis [10] shows that their data are up to 2% higher in the density range from 1100 to 1500 $\text{kg} \cdot \text{m}^{-3}$ (Fig. 6). As shown in Fig. 7, the relative deviations with the data of Ro et al. [11] vary from -2.5 to $+0.5\%$ in the density range 1070 to 1550 $\text{kg} \cdot \text{m}^{-3}$. The data of Gao et al. [12] are slightly lower, and their mean deviations are of the order of -1% in the density range 1000 to 1600 $\text{kg} \cdot \text{m}^{-3}$, corresponding to the temperature range 213 to 333 K (Fig. 8). The mean deviations ($\pm 1.5\%$) of these three sets of data with respect to the values determined by our background equation show that the thermal conductivities can be calculated by Eq. (2) at lower temperatures to 230 K, with comparable uncertainty. It is shown in Fig. 9 that the data of Yata et al. [13] deviate from -4% at $\rho = 1200 \text{ kg} \cdot \text{m}^{-3}$ and $T = 305 \text{ K}$ to $+3\%$ at $\rho = 1500 \text{ kg} \cdot \text{m}^{-3}$ and $T = 257 \text{ K}$, with a mean

Table II. Thermal Conductivity of HFC-125 Along the Quasi-Isotherm 299 K

Temperature (K)	Pressure (MPa)	Density ($\text{kg} \cdot \text{m}^{-3}$)	λ ($\text{mW} \cdot \text{m}^{-1} \cdot \text{K}^{-1}$)
299.27	30.00	1380.8	78.18
299.27	31.00	1384.6	78.59
299.27	32.00	1388.4	79.01
299.27	33.00	1392.2	79.86
299.27	34.00	1395.8	80.73
299.26	35.00	1399.4	81.62
299.26	36.00	1402.8	82.07
299.26	37.00	1406.3	82.52
299.26	38.00	1409.6	82.99
299.25	39.00	1412.9	83.45
299.25	40.00	1416.2	83.92
299.25	41.00	1419.4	84.40
299.25	42.00	1422.5	84.88
299.24	43.00	1425.6	85.37
299.24	44.00	1428.6	85.37
299.24	45.00	1431.6	85.86
299.24	46.00	1434.5	85.86
299.24	47.00	1437.4	86.36
299.24	48.00	1440.2	86.36
299.24	49.00	1443.0	86.86
299.24	50.00	1445.7	86.86
299.24	51.00	1448.5	87.37
299.24	52.00	1451.1	87.37
299.23	53.00	1453.8	87.89

Table III. Thermal Conductivity of HFC-125 Along the Quasi-Isotherm 300 K

Temperature (K)	Pressure (MPa)	Density ($\text{kg} \cdot \text{m}^{-3}$)	λ ($\text{mW} \cdot \text{m}^{-1} \cdot \text{K}^{-1}$)
300.26	5.00	1224.4	61.96
300.24	6.00	1235.1	62.98
300.22	7.00	1244.9	64.02
300.21	8.00	1254.1	64.97
300.20	9.00	1262.6	65.81
300.19	10.00	1270.7	66.67
300.17	11.00	1278.3	67.40
300.16	12.00	1285.5	68.14
300.15	13.00	1292.4	68.90
300.14	14.00	1299.0	69.69
300.13	15.00	1305.3	70.48
300.13	16.00	1311.4	71.13
300.12	17.00	1317.2	71.80
300.10	18.00	1322.9	72.47
300.10	19.00	1328.3	73.16
300.09	20.00	1333.6	73.69
300.09	21.00	1338.6	74.39
300.08	22.00	1343.6	74.94
300.07	23.00	1348.4	75.67
300.07	24.00	1353.0	76.04
300.06	25.00	1357.6	76.61
300.05	26.00	1362.0	77.18
300.05	27.00	1366.3	77.77
300.04	28.00	1370.5	78.35
300.04	29.00	1374.6	78.96
300.03	30.00	1378.6	79.36
300.03	31.00	1382.5	79.98
300.02	32.00	1386.3	80.39
300.02	33.00	1390.0	80.81
300.01	34.00	1393.7	81.24
300.06	35.00	1397.3	81.88
300.00	36.00	1400.8	82.53
300.00	37.00	1404.3	82.98
299.99	38.00	1407.7	83.43
299.99	39.00	1411.0	84.10
299.98	40.00	1414.3	84.34
299.98	41.00	1417.5	84.56
299.98	42.00	1420.6	84.80
299.97	43.00	1423.7	85.26
299.97	44.00	1426.8	85.49
299.97	45.00	1429.8	85.97

Table IV. Thermal Conductivity of HFC-125 Along the Quasi-Isotherm 308.6 K

Temperature (K)	Pressure (MPa)	Density ($\text{kg} \cdot \text{m}^{-3}$)	λ ($\text{mW} \cdot \text{m}^{-1} \cdot \text{K}^{-1}$)
308.75	2.30	1132.0	56.18
308.73	3.10	1147.8	57.17
308.72	4.00	1163.2	58.21
308.70	5.00	1178.1	59.22
308.70	5.90	1190.1	60.06
308.69	6.70	1200.0	60.70
308.67	7.80	1212.2	61.77
308.66	9.00	1224.5	63.00
308.64	10.80	1241.0	64.49
308.62	12.01	1251.1	65.64
308.60	15.00	1273.5	67.70
308.59	16.00	1280.3	68.49
308.58	17.00	1286.8	69.23
308.57	18.00	1293.1	69.98
308.57	19.00	1299.1	70.46
308.56	20.00	1304.9	71.34
308.55	21.00	1310.5	71.90
308.55	22.00	1315.9	72.51
308.54	23.00	1321.2	73.14
308.54	24.00	1326.2	73.62
308.53	25.17	1332.0	74.27
308.53	26.00	1336.0	74.91
308.52	27.00	1340.7	75.47
308.51	28.01	1345.2	76.23
308.51	29.00	1349.6	76.80
308.51	30.00	1353.9	77.11
308.50	31.00	1358.1	77.58
308.50	32.00	1362.3	78.12
308.49	33.00	1366.3	78.60
308.49	34.00	1370.2	79.08
308.48	35.13	1374.5	79.08
308.48	36.00	1377.8	80.16
308.48	37.00	1381.5	80.51
308.47	38.00	1385.1	81.01
308.47	39.00	1388.7	81.60
308.47	39.80	1391.5	81.87

Table V. Thermal Conductivity of HFC-125 Along the Quasi-Isotherm 317 K

Temperature (K)	Pressure (MPa)	Density ($\text{kg} \cdot \text{m}^{-3}$)	λ ($\text{mW} \cdot \text{m}^{-1} \cdot \text{K}^{-1}$)
317.30	3.00	1080.3	53.42
317.29	3.50	1093.6	54.31
317.28	4.00	1105.4	54.91
317.26	4.50	1116.0	55.64
317.25	5.00	1125.7	56.28
317.23	6.00	1142.9	57.49
317.21	7.00	1158.0	58.74
317.19	8.00	1171.5	59.70
317.18	9.00	1183.6	60.56
317.16	10.00	1194.8	61.56
317.15	11.00	1205.7	62.47
317.14	12.00	1214.9	63.40
317.13	13.00	1223.9	64.23
317.11	14.00	1232.4	64.93
317.10	15.00	1240.5	65.80
317.09	16.00	1248.2	66.53
317.08	17.00	1255.5	67.44
317.07	18.00	1262.5	68.21
317.06	19.00	1269.2	68.85
317.06	20.00	1275.6	69.49
317.05	21.00	1281.8	70.15
317.04	22.00	1287.7	70.81
317.04	23.00	1293.5	71.32
317.03	24.00	1299.0	71.84
317.02	25.00	1304.4	72.54
317.02	26.00	1309.6	73.07
317.01	27.00	1314.7	73.61
317.00	28.00	1319.6	74.16
317.00	29.00	1324.4	74.72
317.00	30.00	1329.1	75.10
316.99	31.00	1333.6	75.48
316.99	32.00	1338.0	76.06
316.98	33.00	1342.4	76.45
316.98	34.00	1346.6	77.04
316.97	35.00	1350.7	77.44
316.97	36.00	1354.7	78.05
316.96	37.00	1358.7	78.45
316.96	38.00	1362.5	78.87
316.95	39.00	1366.3	79.29
316.95	40.00	1370.0	79.71
316.95	41.00	1373.6	80.14
316.94	42.00	1377.2	80.57
316.94	43.00	1380.7	81.01
316.93	44.00	1384.1	81.45
316.93	45.00	1387.5	81.89
316.93	46.00	1390.8	82.35

Table VI. Thermal Conductivity of HFC-125 Along the Quasi-Isotherm 317.5 K

Temperature (K)	Pressure (MPa)	Density ($\text{kg} \cdot \text{m}^{-3}$)	λ ($\text{mW} \cdot \text{m}^{-1} \cdot \text{K}^{-1}$)
317.67	3.00	1077.2	52.66
317.65	3.50	1090.8	53.68
317.64	4.00	1102.7	54.34
317.63	4.50	1113.5	55.02
317.62	5.00	1123.3	55.71
317.61	6.00	1140.7	57.00
317.60	7.00	1155.9	58.04
317.58	8.00	1169.5	59.12
317.57	9.00	1181.8	60.09
317.56	10.00	1193.0	60.91
317.54	11.00	1203.4	61.92
317.54	12.00	1213.1	62.80
317.53	13.00	1222.2	63.69
317.52	14.00	1230.8	64.43
317.51	15.00	1238.9	65.38
317.50	16.00	1246.6	65.96
317.49	17.00	1253.9	66.74
317.49	18.00	1261.0	67.34
317.48	19.00	1267.7	68.17
317.47	20.00	1274.2	69.01
317.47	21.00	1280.4	69.65
317.46	22.00	1286.3	70.31
317.46	23.00	1292.0	70.75
317.45	24.00	1297.7	71.20
317.45	25.00	1303.0	71.89
317.44	26.00	1308.3	72.36
317.44	27.00	1313.4	73.06
317.43	28.00	1318.3	73.78
317.43	29.00	1323.1	74.27
317.42	30.00	1327.8	75.02
317.42	31.00	1332.4	75.52
317.41	32.00	1336.8	76.03
317.41	33.00	1341.1	76.55
317.41	34.00	1345.4	76.81
317.40	35.00	1349.5	77.35
317.41	36.00	1353.5	77.88
317.40	37.00	1357.5	78.15
317.40	38.00	1361.4	78.42
317.40	39.00	1365.1	78.70
317.39	40.00	1368.8	78.97
317.39	41.00	1372.5	79.25
317.39	42.00	1376.0	79.53
317.39	43.00	1379.5	79.82
317.38	44.00	1383.0	80.10
317.38	45.00	1386.4	80.39
317.38	46.00	1389.7	80.68
317.38	47.00	1392.9	80.97

Table VII. Thermal Conductivity of HFC-125 Along the Quasi-Isotherm 327.2 K

Temperature (K)	Pressure (MPa)	Density ($\text{kg} \cdot \text{m}^{-3}$)	λ ($\text{mW} \cdot \text{m}^{-1} \cdot \text{K}^{-1}$)
327.62	5.00	1050.5	52.07
327.60	6.00	1075.9	53.57
327.59	7.00	1096.7	54.75
327.57	8.00	1114.5	55.98
327.56	9.00	1130.1	56.98
327.54	10.00	1144.1	58.01
327.53	11.00	1156.8	58.93
327.52	12.00	1168.5	59.87
327.51	13.00	1179.3	60.85
327.50	14.00	1189.3	61.85
327.49	15.00	1198.8	62.71
327.49	16.00	1207.7	63.42
327.47	17.00	1216.1	64.14
327.46	18.00	1224.1	64.88
327.46	19.00	1231.7	65.64
327.45	20.00	1239.0	66.02
327.45	21.00	1245.9	66.41
327.44	22.00	1252.6	67.00
327.44	23.00	1259.0	67.61
327.43	24.00	1265.2	68.43
327.42	25.00	1271.2	69.06
327.42	26.00	1277.0	69.69
327.41	27.00	1282.6	70.35
327.41	28.00	1288.0	71.01
327.40	29.00	1293.3	71.69
327.39	30.00	1298.4	72.38
327.39	31.00	1303.4	73.08
327.39	32.00	1308.2	73.55
327.38	33.00	1312.9	74.03
327.38	34.00	1317.5	74.28
327.38	35.00	1322.0	74.77
327.37	36.00	1326.4	75.26
327.37	37.00	1330.6	75.76
327.38	38.00	1334.8	76.02
327.36	39.00	1338.9	76.53
327.36	40.00	1342.9	76.79
327.36	41.00	1346.8	77.05
327.36	42.00	1350.6	77.31
327.36	43.00	1354.4	77.58
327.35	44.00	1358.0	77.84

Table VIII. Thermal Conductivity of HFC-125 Along the Quasi-Isotherm 375 K

Temperature (K)	Pressure (MPa)	Density ($\text{kg} \cdot \text{m}^{-3}$)	λ ($\text{mW} \cdot \text{m}^{-1} \cdot \text{K}^{-1}$)
375.32	10.00	845.7	45.33
375.31	11.00	884.0	46.73
375.29	12.00	915.1	47.86
375.27	13.00	941.3	49.17
375.25	14.00	964.1	50.42
375.24	15.00	984.2	51.60
375.24	16.00	1002.1	52.83
375.21	17.00	1018.5	54.13
375.87	17.00	1015.6	53.32
375.86	18.00	1030.7	54.30
375.85	19.00	1044.6	55.06
375.84	20.00	1057.6	55.97
375.83	21.00	1069.6	56.77
375.82	22.00	1081.0	57.61
375.81	23.00	1091.7	58.31
375.80	24.00	1101.8	59.18
375.79	25.00	1111.4	59.93
375.79	26.00	1120.6	60.54
375.78	27.00	1129.3	61.31
375.78	28.00	1137.7	62.11
375.76	29.00	1145.8	62.77
375.76	30.00	1153.5	63.44
375.75	31.00	1160.9	63.95
375.75	32.00	1168.1	64.64
375.74	33.00	1175.0	65.17
375.73	34.00	1181.7	65.71
375.73	35.00	1188.1	66.44
375.72	36.00	1194.4	67.00
375.72	37.00	1200.5	67.38
375.72	38.00	1206.4	67.76
375.71	39.00	1212.1	68.14
375.70	40.00	1217.7	68.54
375.70	41.00	1223.1	69.13
375.70	42.00	1228.4	69.53
375.70	43.00	1233.6	69.94
375.69	44.00	1238.6	70.35
375.69	45.00	1243.6	70.76
375.69	46.00	1248.4	70.98
375.69	47.00	1253.1	71.40
375.68	48.00	1257.7	71.82

Table IX. Thermal Conductivity of HFC-125 Along the Quasi-Isotherm 424 K

Temperature (K)	Pressure (MPa)	Density ($\text{kg} \cdot \text{m}^{-3}$)	λ ($\text{mW} \cdot \text{m}^{-1} \cdot \text{K}^{-1}$)
424.36	5.50	245.9	28.25
424.33	6.00	274.8	29.24
424.30	6.50	304.8	30.43
424.27	7.00	335.8	31.54
424.24	7.50	367.6	32.76
424.21	8.00	400.0	33.76
424.19	8.50	432.6	34.76
424.16	9.00	465.0	35.87
424.15	9.50	496.6	36.84
424.14	10.00	527.1	37.41
424.12	10.50	556.3	38.44
424.10	11.00	583.9	39.25
424.08	12.00	634.0	40.71
424.05	13.00	677.9	42.14
424.03	14.00	716.1	43.45
424.02	15.00	749.7	44.57
424.01	16.00	779.4	45.69
423.99	17.00	806.0	46.71
423.98	18.00	829.9	47.63
423.97	19.00	851.5	48.57
423.96	20.00	871.5	49.62
423.95	21.00	889.9	50.50
423.94	22.00	906.9	51.43
423.93	23.00	922.7	52.35
423.92	24.00	937.5	53.37
423.91	25.00	951.4	53.92
423.91	26.00	964.6	54.61
423.90	27.00	977.0	55.31
423.89	28.00	988.7	56.28
423.89	29.00	1000.0	57.03
423.89	30.00	1010.6	57.62
423.88	31.00	1020.9	58.18
423.88	32.00	1030.7	59.02
423.87	33.00	1040.1	59.50
423.86	34.00	1049.1	60.12
423.86	35.00	1057.8	60.76
423.86	36.00	1066.2	61.26
423.85	37.00	1074.3	61.93
423.85	38.00	1082.1	62.62
423.85	39.00	1089.7	63.05
423.84	40.00	1097.0	63.57
423.84	41.00	1104.1	63.90
423.84	42.00	1111.0	64.37
423.83	43.00	1118.1	64.85
423.83	44.00	1124.2	65.42
423.83	45.00	1130.6	65.92
423.82	46.00	1136.8	66.45
423.82	47.00	1142.8	66.94

Table X. Thermal Conductivity of HFC-125 Along the Quasi-Isotherm 433 K

Temperature (K)	Pressure (MPa)	Density ($\text{kg} \cdot \text{m}^{-3}$)	λ ($\text{mW} \cdot \text{m}^{-1} \cdot \text{K}^{-1}$)
433.52	0.1	3.3	25.41
433.51	1.00	34.9	25.88
433.49	2.00	73.0	26.67
433.47	3.00	114.6	27.39
433.45	4.00	159.7	28.27
433.43	5.00	208.3	29.30
433.41	6.00	260.4	30.46
433.38	7.00	315.7	32.08
433.35	8.00	373.4	33.97
433.32	9.00	432.0	36.19
433.30	10.00	489.3	37.71
433.28	11.00	543.2	39.23
433.26	12.00	592.3	40.73
433.24	13.00	636.3	42.19
433.23	14.00	675.4	43.59
433.22	15.00	710.0	44.75
433.21	16.00	741.0	45.97
433.20	17.00	768.8	46.88
433.19	18.00	794.0	48.01
433.19	19.00	816.8	48.81
433.18	20.00	837.8	49.83
433.17	21.00	857.2	50.67
433.17	22.00	875.1	51.33
433.16	23.00	891.7	52.00
433.16	24.00	907.3	52.69
433.15	25.00	922.0	53.40
433.15	26.00	935.8	54.12
433.15	27.00	948.9	54.87
433.14	28.00	961.2	55.38
433.14	29.00	973.0	55.89
433.13	30.00	984.2	56.69
433.13	31.00	995.0	57.23
433.13	32.00	1005.2	57.78
433.13	33.00	1015.0	58.34
433.12	34.00	1024.5	58.91
433.12	35.00	1033.6	59.49
433.12	36.00	1042.4	60.09
433.11	37.00	1050.9	60.69
433.11	38.00	1059.0	61.31
433.10	39.00	1067.0	61.94
433.10	40.00	1074.6	62.60
433.10	41.00	1082.0	62.91
433.10	42.00	1089.2	63.25
433.10	43.00	1096.2	63.58
433.10	44.00	1103.0	63.92
433.10	45.00	1109.7	63.92
433.10	46.00	1116.1	64.26
433.10	47.00	1122.4	64.26

Table XI. Thermal Conductivity of HFC-125 Along the Quasi-Isotherm 453 K

Temperature (K)	Pressure (MPa)	Density ($\text{kg} \cdot \text{m}^{-3}$)	λ ($\text{mW} \cdot \text{m}^{-1} \cdot \text{K}^{-1}$)
453.41	0.1	3.2	27.07
453.40	1.00	33.1	27.30
453.39	2.00	68.9	27.66
453.37	3.00	107.1	28.29
453.35	4.00	147.9	29.04
453.32	5.00	190.8	29.95
453.30	6.00	235.7	31.02
453.26	7.00	282.4	32.10
453.24	8.00	330.2	33.47
453.20	9.00	378.7	34.94
453.18	10.00	427.0	36.39
453.15	11.00	473.9	38.04
453.12	12.00	518.6	39.38
453.10	13.00	560.3	40.61
453.08	14.00	598.7	41.82
453.07	15.00	633.9	42.88
453.06	16.00	666.0	44.00
453.04	17.00	695.3	44.93
453.03	18.00	722.1	46.15
453.01	19.00	746.8	47.17
453.00	20.00	769.5	48.10
453.00	21.00	790.5	49.07
452.99	22.00	810.0	49.93
452.98	23.00	828.3	50.83
452.97	24.00	845.3	51.60
452.96	25.00	861.4	52.38
452.96	26.00	876.5	53.03
452.95	27.00	890.8	53.70
452.94	28.00	904.4	54.20
452.94	29.00	917.2	54.89
452.93	30.00	929.5	55.43
452.93	31.00	941.2	55.78
452.93	32.00	952.4	56.33
452.92	33.00	963.2	56.70
452.92	34.00	973.5	57.27
452.92	35.00	983.4	57.85
452.91	36.00	993.0	58.43
452.90	37.00	1002.2	59.03
452.91	38.00	1011.1	59.65
452.90	39.00	1019.7	60.27
452.89	40.00	1028.0	60.69
452.89	41.00	1036.1	61.34
452.88	42.00	1043.9	62.00
452.88	43.00	1051.6	62.45
452.88	44.00	1058.9	62.90
452.88	45.00	1066.1	63.36
452.87	46.00	1073.0	63.83
452.87	47.00	1079.8	64.30

Table XII. Thermal Conductivity of HFC-125 Along the Quasi-Isotherm 463 K

Temperature (K)	Pressure (MPa)	Density ($\text{kg} \cdot \text{m}^{-3}$)	λ ($\text{mW} \cdot \text{m}^{-1} \cdot \text{K}^{-1}$)
463.28	0.1	3.13	27.63
463.27	1.00	32.3	27.86
463.25	2.00	67.0	28.35
463.24	3.00	103.9	29.05
463.22	4.00	142.8	29.74
463.19	5.00	183.6	30.57
463.17	6.00	225.9	31.44
463.14	7.00	269.4	32.64
463.12	8.00	313.8	33.82
463.08	9.00	358.7	35.40
463.05	10.00	403.3	36.81
463.03	11.00	447.1	38.23
463.01	12.00	489.1	39.49
462.99	13.00	529.1	40.53
462.97	14.00	566.4	41.92
462.96	15.00	601.0	42.41
462.94	16.00	633.0	43.90
462.93	17.00	662.4	44.95
462.92	18.00	689.6	45.92
462.90	19.00	714.7	46.94
462.90	20.00	737.9	47.72
462.89	21.00	759.5	48.54
462.88	22.00	779.6	49.47
462.87	23.00	798.4	50.05
462.87	24.00	816.0	50.55
462.86	25.00	832.6	51.31
462.86	26.00	848.3	51.93
462.85	27.00	863.1	52.57
462.84	28.00	877.1	53.22
462.84	29.00	890.5	53.89
462.83	30.00	903.2	54.67
462.83	31.00	915.4	55.37
462.82	32.00	927.0	55.99
462.81	33.00	938.2	56.73
462.81	34.00	948.9	57.49
462.80	35.00	959.2	58.07
462.80	36.00	969.1	58.66
462.79	37.00	978.7	59.06
462.79	38.00	987.9	59.58
462.79	39.00	996.8	59.99
462.79	40.00	1005.5	60.30
462.79	41.00	1013.8	60.72
462.78	42.00	1021.9	61.15
462.78	43.00	1029.8	61.59
462.78	44.00	1037.4	62.04
462.77	45.00	1044.9	62.48
462.77	46.00	1052.0	63.04
462.77	47.00	1059.1	63.39

Table XIII. Thermal Conductivity of HFC-125 Along the Quasi-Isotherm 473 K

Temperature (K)	Pressure (MPa)	Density ($\text{kg} \cdot \text{m}^{-3}$)	λ ($\text{mW} \cdot \text{m}^{-1} \cdot \text{K}^{-1}$)
473.73	0.1	3.06	28.53
473.72	1.00	31.5	29.10
473.71	2.00	65.1	29.57
473.69	3.00	100.7	30.11
473.67	4.00	138.0	30.79
473.65	5.00	176.8	31.67
473.63	6.00	216.7	32.52
473.60	7.00	257.5	33.43
473.59	8.00	298.9	34.39
473.56	9.00	340.5	35.60
473.55	10.00	381.9	36.53
473.52	11.00	422.7	37.62
473.51	12.00	462.2	38.66
473.49	13.00	500.1	39.85
473.47	14.00	536.0	40.99
473.45	15.00	569.7	42.02
473.44	16.00	601.1	42.99
473.43	17.00	630.4	44.00
473.42	18.00	657.6	45.47
473.40	19.00	682.8	46.16
473.39	20.00	706.4	46.92
473.39	21.00	728.4	47.85
473.37	22.00	748.9	48.64
473.36	23.00	768.2	49.37
473.36	24.00	786.3	49.98
473.35	25.00	803.4	50.57
473.35	26.00	819.5	51.35
473.34	27.00	834.8	52.23
473.34	28.00	849.3	53.04
473.33	29.00	863.1	53.71
473.32	30.00	876.0	54.36
473.32	31.00	888.8	54.92
473.31	32.00	900.9	55.50
473.31	33.00	912.4	56.05
473.30	34.00	923.5	56.60
473.30	35.00	934.2	57.47
473.30	36.00	944.4	57.86
473.30	37.00	954.3	58.25
473.29	38.00	963.9	58.61
473.28	39.00	973.1	58.87
473.28	40.00	982.1	59.35
473.28	41.00	990.7	60.51
473.27	42.00	999.1	60.60
473.27	43.00	1007.3	61.35
473.27	44.00	1015.1	61.79
473.26	45.00	1022.9	62.01
473.26	46.00	1030.3	62.65
473.25	47.00	1037.6	62.96

Table XIV. Thermal Conductivity of HFC-125 Along the Quasi-Isotherm 493 K

Temperature (K)	Pressure (MPa)	Density ($\text{kg} \cdot \text{m}^{-3}$)	λ ($\text{mW} \cdot \text{m}^{-1} \cdot \text{K}^{-1}$)
493.31	0.10	2.94	30.25
493.30	1.00	30.2	30.64
493.29	2.00	62.0	31.04
493.28	3.00	95.4	31.63
493.27	4.00	130.0	32.23
493.25	5.00	165.7	32.87
493.24	6.00	202.1	33.52
493.22	7.00	238.8	34.41
493.20	8.00	275.8	35.35
493.18	9.00	312.8	36.26
493.16	10.00	349.5	37.22
493.15	11.00	385.7	38.22
493.13	12.00	421.0	39.28
493.11	13.00	455.4	40.40
493.10	14.00	488.3	41.48
493.08	15.00	519.8	42.41
493.06	16.00	549.7	43.48
493.06	17.00	577.9	44.39
493.05	18.00	604.5	45.32
493.04	19.00	629.6	46.17
493.02	20.00	653.2	46.92
493.01	21.00	675.4	47.71
493.01	22.00	696.3	48.37
493.00	23.00	716.0	49.19
492.99	24.00	734.7	49.90
492.99	25.00	752.3	50.63
492.98	26.00	769.1	51.39
492.98	27.00	785.0	51.85
492.97	28.00	800.2	52.63
492.96	29.00	814.6	53.11
492.96	30.00	828.4	53.77
492.95	31.00	841.6	54.45
492.95	32.00	854.3	54.96
492.94	33.00	866.4	55.49
492.94	34.00	878.1	56.02
492.94	35.00	889.4	56.38
492.9	36.00	900.2	56.94
492.93	37.00	910.6	57.50
492.92	38.00	920.7	58.07
492.92	39.00	930.5	58.46
492.91	40.00	939.9	59.05
492.91	41.00	949.1	59.46
492.91	42.00	958.0	59.87
492.91	43.00	966.6	60.48
492.90	44.00	975.0	61.12
492.90	45.00	983.1	61.55
492.90	46.00	991.1	61.98
492.89	47.00	998.7	62.42

Table XV. Thermal Conductivity of HFC-125 Along the Quasi-Isotherm 513 K

Temperature (K)	Pressure (MPa)	Density ($\text{kg} \cdot \text{m}^{-3}$)	λ ($\text{mW} \cdot \text{m}^{-1} \cdot \text{K}^{-1}$)
513.21	0.10	2.82	32.00
513.21	1.00	28.9	32.25
513.20	2.00	59.2	32.57
513.19	3.00	90.7	32.96
513.18	4.00	123.1	33.49
513.17	5.00	156.2	34.04
513.16	6.00	189.7	34.76
513.14	7.00	223.4	35.50
513.13	8.00	257.0	36.27
513.11	9.00	290.5	37.08
513.10	10.00	323.7	37.92
513.09	11.00	356.3	38.71
513.08	12.00	388.3	39.62
513.06	13.00	419.5	40.58
513.04	14.00	449.7	41.58
513.03	15.00	478.8	42.42
513.02	16.00	506.8	43.29
513.00	17.00	533.5	44.19
513.00	18.00	559.0	44.90
512.99	19.00	583.3	45.50
512.98	20.00	606.4	46.62
513.18	21.00	628.3	47.27
512.96	22.00	649.1	48.07
512.96	23.00	668.8	48.76
512.95	24.00	687.6	49.47
512.94	25.00	705.5	50.05
512.94	26.00	722.6	50.79
512.93	27.00	738.8	51.40
512.92	28.00	754.4	52.19
512.92	29.00	769.2	52.83
512.91	30.00	783.5	53.33
512.91	31.00	797.1	54.00
512.90	32.00	810.2	54.69
512.90	33.00	822.8	55.21
512.90	34.00	835.0	55.75
512.89	35.00	846.6	56.30
512.89	36.00	857.9	56.86
512.88	37.00	868.8	57.43
512.88	38.00	879.4	58.01
512.87	39.00	889.5	58.41
512.87	40.00	899.4	59.01
512.87	41.00	909.0	59.41
512.86	42.00	918.3	59.82
512.86	43.00	927.3	60.45
512.86	44.00	936.1	60.88
512.85	45.00	944.6	61.31
512.85	46.00	952.9	61.75
512.85	47.00	961.0	62.19

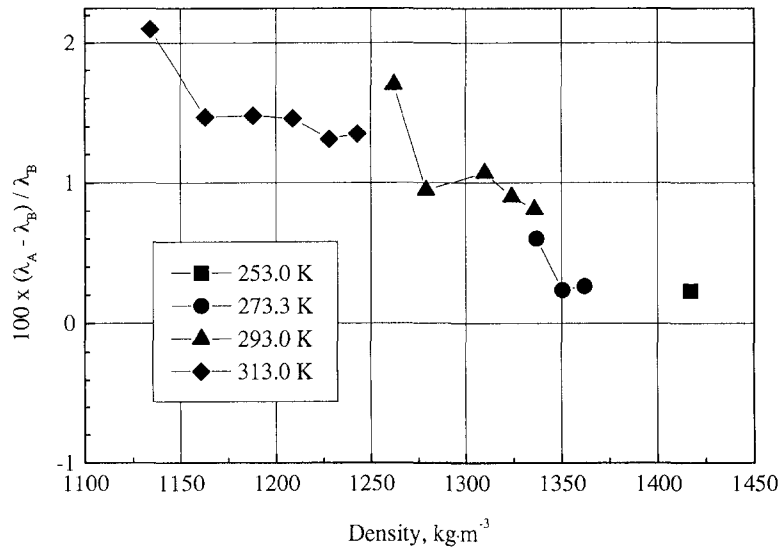


Fig. 6. Relative deviations between the experimental data of Assael and Karagiannidis [10] and the values calculated by the background equation.

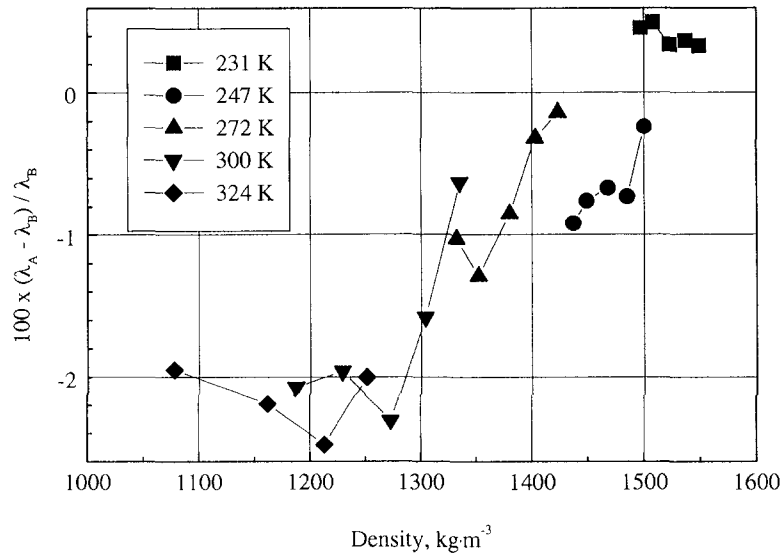


Fig. 7. Relative deviations between the experimental data of Ro et al. [11] and the values calculated by the background equation.

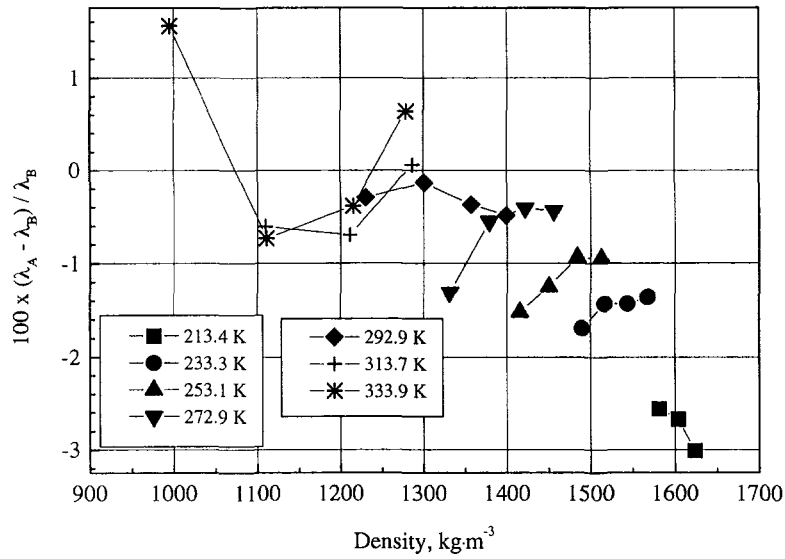


Fig. 8. Relative deviations between the data of Gao et al. [12] and the values calculated by the background equation.

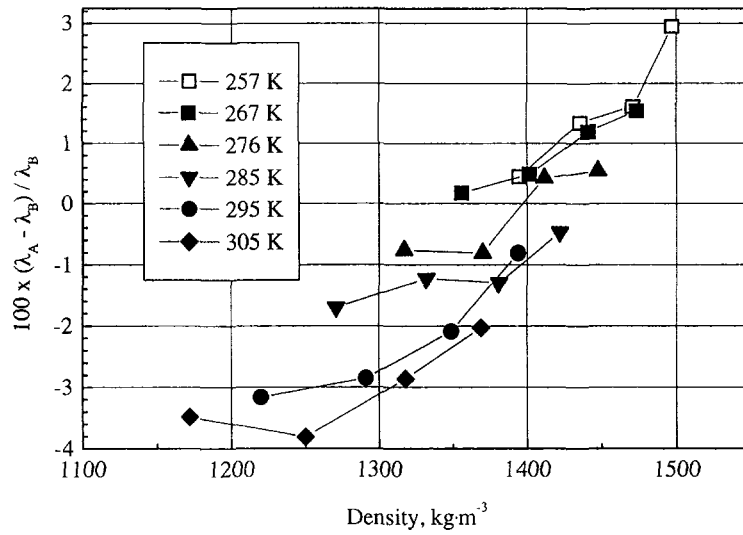


Fig. 9. Relative deviations between the experimental data of Yata et al. [13] and the values calculated by the background equation.

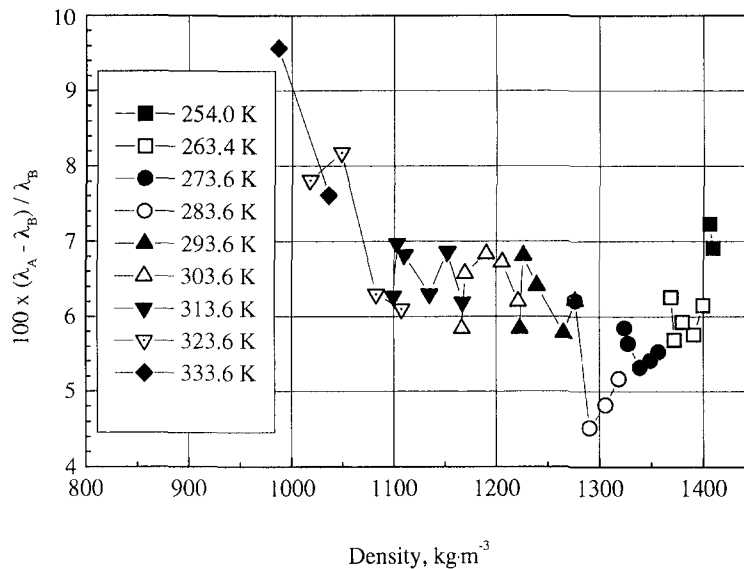


Fig. 10. Relative deviations of the experimental data of Gross and Song [14] from the values calculated with the background equation.

deviation of $\pm 2\%$. The comparison with the data of Gross and Song [14] shows that there is a systematic deviation with their data, which are about 6% higher than those from this work (Fig. 10). Along the saturation curve, the deviations with the data of Tsvetkov et al. [15] vary from -0.3% at 226 K to $+6.1\%$ at 290 K.

5. CONCLUSION

New measurements of the thermal conductivity of HFC-125 are presented in the temperature range from 300 to 515 K along 14 quasi-isotherms and at pressures up to 53 MPa, with an estimated uncertainty of $\pm 1.5\%$. A background equation was determined which can be used to calculate the thermal conductivity from 220 to 600 K with an uncertainty of $\pm 2\%$. It is obvious that in the critical region a supplementary functional form must be added to take into account the critical enhancement which influences the thermal conductivity far away from the critical point

ACKNOWLEDGMENT

We are indebted to Elf Atochem for providing us HFC-125 samples.

REFERENCES

1. S. L. Outcalt and M. O. McLinden, *Int. J. Thermophys.* **16**:79 (1995).
2. A. T. Sousa, P. S. Fialho, C. A. Nieto de Castro, R. Tufeu, and B. Le Neindre, *Int. J. Thermophys.* **13**:363 (1992).
3. B. Le Neindre and R. Tufeu, in *Experimental Thermodynamics III, Measurements of the Transport Properties of Fluids*, W. A. Wakeham, A. Nagashima, and J. V. Sengers, eds. (Blackwell, Oxford, 1991), pp. 111–142.
4. L. C. Wilson, W. V. Wilding, G. M. Wilson, R. L. Rowley, V. M. Felix, and T. Chisolm-Carter, *Fluid Phase Equil.* **80**:167 (1992).
5. M. J. Assael and S. K. Polimatidou, *Int. J. Thermophys.* **18**:353 (1997).
6. C. M. B. P. Oliveira and W. A. Wakeham, *Int. J. Thermophys.* **14**:1131 (1993).
7. A. Yokozeki, H. Sato, and K. Watanabe, *Int. J. Thermophys.* **19**:89 (1998).
8. M. J. Assael, N. Malamataris, and L. Karagiannidis, *Int. J. Thermophys.* **18**:341 (1997).
9. Y. Tanaka, S. Matsuo, and S. Taya, *Int. J. Thermophys.* **16**:121 (1995).
10. M. J. Assael and L. Karagiannidis, *Int. J. Thermophys.* **16**:851 (1995).
11. S. T. Ro, M. S. Kim, and S. U. Jeong, *Int. J. Thermophys.* **18**:991 (1997).
12. X. Gao, T. Yamada, Y. Nagasaka, and A. Nagashima, *Int. J. Thermophys.* **17**:279 (1996).
13. J. Yata, M. Hori, K. Kobayashi, and T. Minamiyama, *Int. J. Thermophys.* **17**:561 (1996).
14. U. Gross and Y. W. Song, *Int. J. Thermophys.* **17**:607 (1996).
15. O. B. Tsvetkov, Yu. A. Laptev, and A. G. Asambaev, *Int. J. Thermophys.* **15**:203 (1994).